

Performance Analysis of a RED-MED Salinity Gradient Heat Engine

Patricia Palenzuela ¹, Marina Micari ^{2,3}, Bartolomé Ortega-Delgado ², Francesco Giacalone ², Guillermo Zaragoza ¹, Diego-César Alarcón-Padilla ¹, Andrea Cipollina ^{2,*}, Alessandro Tamburini ² and Giorgio Micale ²

¹ CIEMAT-Plataforma Solar de Almería, Ctra. de Senés s/n, 04200 Tabernas, Almería, Spain;

patricia.palenzuela@psa.es (P.P.); guillermo.zaragoza@psa.es (G.Z.); diego.alarcon@psa.es (D.-C.A.-P.);

² DIID—Dipartimento dell’Innovazione Industriale e Digitale—Ingegneria Chimica, Gestionale, Informatica, Meccanica, Università degli Studi di Palermo (UNIPA), viale delle Scienze, Ed. 6, 90128 Palermo, Italy; marina.micari@dlr.de (M.M.); bartolome.ortegadelgado@unipa.it (B.O.-D.); francesco.giacalone07@unipa.it (F.G.); alessandro.tamburini@unipa.it (A.T.); giorgiod.maria.micale@unipa.it (G.M.)

³ German Aerospace Center (DLR), Institute of Engineering Thermodynamics, Pfaffenwaldring 38-40, 70569 Stuttgart, Germany

* Correspondence: andrea.cipollina@unipa.it; Tel.: +3909123863788

Received: 5 October 2018; Accepted: 20 November 2018; Published: date

S1. Description and modelling of the systems

Reverse Electrodialysis process

The reverse electrodialysis process has been modelled, following a hierarchical approach. The low-hierarchy model describes one cell pair and contains the equations to calculate all the thermodynamic and physical properties, the fluxes through the membrane, the flow rates and concentration along the channel and the electrical variables. The equations are reported in Table S1.1. The electric behaviour of the solution is governed by the generation of the electromotive force inside the RED stack and by the stack electrical resistance, which are calculated via Equations S1.1 and S1.2. $E_{cell}(x)$ is affected by the permselectivity (α_{av}) [1,2] and the polarisation coefficients ($\theta_H(x)$ and $\theta_L(x)$) (Equation S1.1), which influence the concentration at the membrane/solution interface [3]. Correlations for α_{av} and θ are reported in Section S2. The resistance of the cell pair $R_{cell}(x)$ (Equation S1.2) is composed by the resistance of the ion selective membranes ($R_{AEM}(x)$ and $R_{CEM}(x)$), dilute channel ($R_L(x)$) and concentrate channel ($R_H(x)$). The first two terms, i.e., $R_{AEM}(x)$ and $R_{CEM}(x)$, are estimated through empirical correlations derived from experimental data obtained for FujiFilm® membranes (see Section S2). Finally, the variation of solutions concentration and flow rate along the channels can be described through the differential balance equations (Equations S1.4–S1.7). These strongly depend on: (i) the total salt flux given by the sum of coulombic (J_{coul}) and diffusive (J_{diff}) fluxes, defined in Equations S1.8 and S1.9 respectively; (ii) the total water flux, given by the sum of osmotic (J_{osm}) and electro-osmotic (J_{eos}) fluxes, defined in Equations S1.10 and S1.11 respectively.

Table S1.1 Relevant equations for the low-hierarchy RED model.

Equation	Short description
$E_{cell}(x) = 2 \alpha_{av} \frac{R_u T}{F} \ln \left(\theta_H(x) \cdot \theta_L(x) \frac{\gamma_H(x) C_H(x)}{\gamma_L(x) C_L(x)} \right)$	(S1.1) Electro motive force generated by the cell pair (Nernst’s equation [4,5])
$R_{cell}(x) = R_{AEM}(x) + R_{CEM}(x) + R_H(x) + R_L(x)$	(S1.2) Electrical resistance of the cell pair
$R_{sol}(x) = sf \cdot \frac{\delta_{channel}}{A_{sol}(x) \cdot C_{sol}(x)}$	(S1.3) Electrical resistance of the solution compartments [6]

$$\frac{dC_L(x)}{dx} = \frac{b}{Q_L} (J_{diff}(x) + J_{coul}(x)) - C_L(x) \frac{b}{Q_L} (J_{eos}(x) + J_{osm}(x)) \quad (S1.4)$$
 Salinity balance in the dilute compartment [7]

$$\frac{dC_H(x)}{dx} = -\frac{b}{Q_H} (J_{diff}(x) + J_{coul}(x)) + C_H(x) \frac{b}{Q_H} (J_{eos}(x) + J_{osm}(x)) \quad (S1.5)$$
 Salinity balance in the concentrate compartment [7]

$$\frac{dQ_L(x)}{dx} = -(J_{eos}(x) + J_{osm}(x)) \cdot b \cdot \frac{M_w}{\rho_w} \quad (S1.6)$$
 Volume flow rate balance in the dilute compartment [7]

$$\frac{dQ_H(x)}{dx} = -(J_{eos}(x) + J_{osm}(x)) \cdot b \cdot \frac{M_w}{\rho_w} \quad (S1.7)$$
 Volume flow rate balance in the concentrate compartment [7]

$$J_{coul}(x) = \frac{j(x)}{F} \quad (S1.8)$$
 Migrative (or coulombic) flux across the membrane

$$J_{diff}(x) = 2 \frac{D_s}{\delta_m} [C_H(x) - C_L(x)] \quad (S1.9)$$
 Diffusive flux across the membrane (D_s constant and equal to 10^{-12} m²/s [8])

$$J_{osm}(x) = -2L_P \Delta \Pi = -2L_P [vR_u T (\varphi_H(x)C_H(x) - \varphi_L(x)C_L(x))] \cdot \frac{\rho_w}{M_w} \quad (S1.10)$$
 Osmotic water flux across the membrane (v is the Van't Hoff factor, equal to 2 for NaCl salt solution)

$$J_{eos}(x) = n_h \cdot J_{tot}(x) \quad (S1.11)$$
 Electro-osmotic water flux across the membrane (n_h is the total hydration number for the cation and the anion, equal to 7 for the case of Na⁺ and Cl⁻ [9])

The high-hierarchy model describes the whole RED stack and it allows the calculation of global stack variables such as the stack voltage, the electric current, the stack resistance and the power density. The relevant equations are reported in Table S1.2. Channel length is subdivided in a certain number of computational elements ($N_k=50$). Each element is considered as a branch of an electrical circuit containing a generator and a resistance in series. All branches are in parallel, exposed to the same voltage difference (i.e. the electrodes voltage E_{stack} , calculated in Equation (S1.14)). A current $I_{cell}(x)$ is associated to each branch, which is evaluated through the Kirchhoff's loop rule, Eq. (S1.12). Conversely, I_{stack} is given by the Kirchhoff's nodal rule, summing all the currents $I_{cell}(x)$, which converge to the same node, Equation (S1.13). The model also allows calculating the pressure drops along the channels, which are taken into account to calculate the pumping power needed to circulate the feed solutions and, then, the net power generated by the RED unit (Equations S1.17–S1.19).

Table S1.2 Relevant equations for the high-hierarchy RED model

Equation	Short Description
$I_{cell}(x) = \frac{N \cdot E_{cell}(x) - \left(E_{stack} + \frac{R_{blank}}{A} I_{stack} \right)}{N R_{cell}(x)} \quad (S1.12)$	Electric current associated to each branch of the electric circuit
$I_{stack} = \sum_0^L I_{cell}(x) \quad (S1.13)$	Stack electric current
$E_{stack} = R_{ext} I_{stack} \quad (S1.14)$	Stack voltage generated at the ends of the external load R_{ext}
$P_{out,gross} = E_{stack} I_{stack} \quad (S1.15)$	Gross power generated by the stack

$$P_{d,gross} = \frac{P_{out,gross}}{N \cdot A} \quad (S1.16) \quad \text{Gross power density generated by the stack}$$

$$P_{pumping,RED} = P_{pumping,H} + P_{pumping,L} = \frac{\Delta p_H Q_H}{\eta_{pump}} + \frac{\Delta p_L Q_L}{\eta_{pump}} \quad (S1.17) \quad \text{Pumping power required by the RED stack, depending on their geometry and on the Reynolds number [10]}$$

$$P_{out,net} = P_{out,gross} - P_{pumping,RED} \quad (S1.18) \quad \text{Net power produced by the RED stack}$$

$$P_{D,net} = \frac{P_{out,net}}{N \cdot A} \quad (S1.19) \quad \text{Net power density produced by the RED stack}$$

Multi-effect distillation process

A brief resume of the most significant equations of the cited MED model is presented in Table S1.3.

Table S1.3. Brief resume of MED-FF model. The complete model is described in [11].

Equation	Short Description
$T_i = T_{Vi} = T_{Vsat,i} + BPE_i$ (S1.20)	Temperature of the concentrated solution and vapour in each effect
$T_{c,i} = T_{Vi} - BPE_i - (\Delta T_{demister,i} + \Delta T_{lines,i} + \Delta T_{cond,i})$ (S1.21)	Condensation temperature of the vapour generated in the effect i
$\dot{m}_F = \dot{m}_{B1} + \dot{m}_{T1}$ (S1.22)	Mass balance in the first effect
$\dot{m}_F X_F = \dot{m}_{B1} X_1$ (S1.23)	Salinity balance in the first effect
$\dot{m}_s \lambda_s + \dot{m}_F h_{preh2} = (1 - \alpha_1) \dot{m}_{T1} h'_{V1} + \alpha_1 \dot{m}_{T1} h'_{C1} + \dot{m}_{B1} h_{B1}$ (S1.24)	Energy balance in the first effect
$P_{Q1} = \dot{m}_F \bar{c}_{p1} (T_1 - t_{preh1}) + \dot{m}_{D1} \lambda_{V1} = A_1 U_{e1} (T_s - T_1)$ (S1.25)	Heat transfer equation in the first evaporator
$\dot{m}_F \bar{c}_{p,preh1} (t_{preh1} - t_{preh2}) = \alpha_1 \dot{m}_{T1} \lambda'_{V1} + \alpha_1 \dot{m}_{T1} \bar{c}_{p,BPE1} (T'_{V1} - T'_{Vsat1})$ (S1.26)	Energy balance in preheater 1
$\dot{m}_{C1} h''_{C1} + (1 - \alpha_1) \dot{m}_{T1} h_{C1} + \alpha_2 \dot{m}_{T2} h'_{C2} = \dot{m}_{FB2} h''_{V2} + \dot{m}_{C2} h''_{C2}$ (S1.27)	Energy balance in flash box 2

S2. Thermodynamic and physical properties of salt solutions and IEMs

Pitzer's model for activity and osmotic coefficients

The thermodynamic and physical properties of a monovalent salt in water solution are estimated through the Pitzer's model for single salt-water solutions [12–14]. The equations are reported below:

$$\varphi(x) - 1 = -A_\phi \cdot \frac{\sqrt{m_{\text{salt}}(x)}}{1 + B\sqrt{m_{\text{salt}}(x)}} + m_{\text{salt}}(x) \cdot B^\phi(x) + m_{\text{salt}}(x)^2 \cdot C^\phi \quad (\text{S2.1})$$

$$B^\phi(x) = \beta^{(0)} + \beta^{(1)} e^{-\alpha\sqrt{m_{\text{salt}}(x)}} \quad (\text{S2.2})$$

$$\gamma_{\text{salt}}(x) = \gamma_{\text{an}}(x) = \gamma_{\text{cat}}(x) = \exp(f_\gamma(x) + m_{\text{salt}}(x) \cdot B_\gamma(x) + m_{\text{salt}}(x)^2 \cdot C^\gamma) \quad (\text{S2.3})$$

$$f_\gamma(x) = -A_\phi \left[\frac{\sqrt{m_{\text{salt}}(x)}}{1 + B\sqrt{m_{\text{salt}}(x)}} + \frac{2}{B} \cdot \ln(1 + B\sqrt{m_{\text{salt}}(x)}) \right] \quad (\text{S2.4})$$

$$B_\gamma(x) = 2\beta^{(0)} + 2\beta^{(1)} \frac{\left(1 - \left(1 + \alpha\sqrt{m_{\text{salt}}(x)} - \alpha^2 \frac{m_{\text{salt}}(x)}{2}\right) \exp(-\alpha\sqrt{m_{\text{salt}}(x)})\right)}{\alpha^2 m_{\text{salt}}(x)} \quad (\text{S2.5})$$

$$C^\gamma = \frac{3}{2} C^\phi \quad (\text{S2.6})$$

where $\varphi(x)$ is the osmotic coefficient, A_ϕ , α and B are Pitzer's model parameters, $m_{\text{salt}}(x)$ is the molality of the salt, $\beta^{(0)}$, $\beta^{(1)}$ and C^ϕ are specific parameters for each salt, $\gamma_{\text{salt}}(x)$, $\gamma_{\text{cat}}(x)$ and $\gamma_{\text{an}}(x)$ are the salt, cations and anions activity coefficients, respectively.

Equivalent conductivity of salt solutions

The equivalent conductivity of salt solutions has been evaluated through the Jone and Dole's equation [15]:

$$\Lambda_{\text{sol}}(x) = \Lambda_0 - \frac{A_\Lambda \sqrt{C_{\text{sol}}(x)}}{1 + B_\Lambda \sqrt{C_{\text{sol}}(x)}} - C_\Lambda \cdot C_{\text{sol}}(x) \quad (\text{S2.7})$$

where Λ_0 is the equivalent conductivity of the salt at infinite dilution, $C_{\text{sol}}(x)$ is the molar concentration of the solution, and A_Λ , B_Λ and C_Λ are specific parameters for each salt.

IEMs electrical resistance

IEMs electrical resistance has been calculated through empirical correlations derived from experimental data obtained for FujiFilm® membranes [16] (E1 type, thickness of 250 μm):

$$R_{\text{AEM}}(x) = 0.487 \cdot C_{\text{H}}^2(x) - 2.81 \cdot C_{\text{H}}(x) + 7.21 - 0.14 \cdot C_{\text{L}}(x) \quad (\text{S2.8})$$

$$R_{\text{CEM}}(x) = 0.487 \cdot C_{\text{H}}^2(x) - 2.81 \cdot C_{\text{H}}(x) + 7.22 - 0.27 \cdot C_{\text{L}}(x) \quad (\text{S2.9})$$

where $C_{\text{H}}(x)$ and $C_{\text{L}}(x)$ are the molar concentrations of the concentrate and the dilute solution, respectively.

IEMs permselectivity

The membrane permselectivity was evaluated through empirical correlations, derived for the same membranes (FujiFilm® E1 type membranes):

$$\alpha_{AEM}(x) = 0.987 - 0.0441 \cdot C_H(x) - 0.183 \cdot C_L(x) \quad (S2.10)$$

$$\alpha_{CEM}(x) = 0.991 - 0.0441 \cdot C_H(x) - 0.253 \cdot C_L(x) \quad (S2.11)$$

Polarisation coefficients and Sherwood numbers

The polarisation coefficients were calculated implementing suitable correlations, obtained through CFD simulations for the case of flat membranes and Deukum[®] spacers [17].

$$\theta_L(x) = \left(1 + \left(\frac{2 J_s(x) \delta_L}{Sh_L(x) D_L C_L(x)} \right) \right)^{-1} \quad (S2.12)$$

$$\theta_H(x) = 1 - \left(\frac{2 J_s(x) \delta_H}{Sh_H(x) D_H C_H(x)} \right) \quad (S2.13)$$

where δ_H and δ_L are the thicknesses of the spacers used in the concentrate and in the dilute channel respectively; D_H and D_L are the salt diffusivity values in the concentrate and in the dilute channel respectively, considered constant and equal to 1.5×10^{-9} m²/s; Sh_H and Sh_L are the Sherwood numbers, relevant to the concentrate and the dilute solutions, which are calculated as functions of the Reynolds numbers Re_H and Re_L , respectively [3], and the Schmidt number Sc (Sc_{ref} for 25 °C, 1 atm and 0.017 M).

$$Sh(x) = (-1.481 \cdot 10^{-7} Re(x)^5 + 3.739 \cdot 10^{-5} Re(x)^4 - 3.253 \cdot 10^{-3} Re(x)^3 + 1.117 \cdot 10^{-1} Re(x)^2 + 1.348 \cdot 10^{-1} Re(x) + 6.954) \cdot \left(\frac{Sc(x)}{Sc_{ref}(x)} \right)^{0.5} \quad (S2.14)$$

Boiling point elevation (BPE)

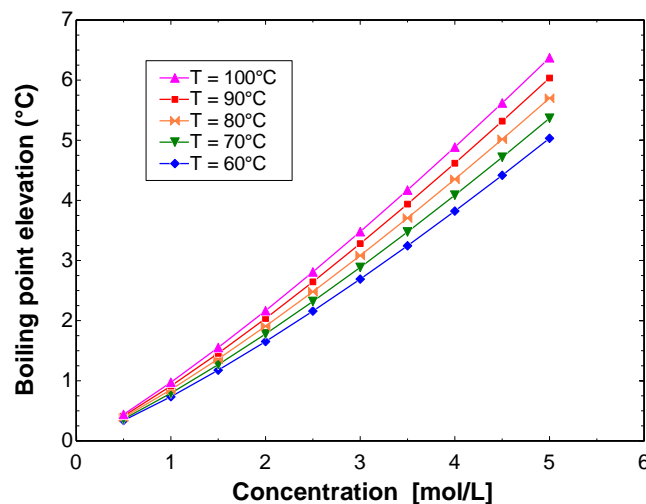


Figure S2.1. Variation of the boiling point elevation of NaCl with salt concentration for different equilibrium vapour temperatures.

S3. MED performance and pumping power consumption

MED performance: correlation parameters

Table S3.1. Parameters of the fitting equations for the specific thermal consumption and number of effects of the MED unit (referring to waste-heat temperature of 100 °C, giving the lowest *STC*).

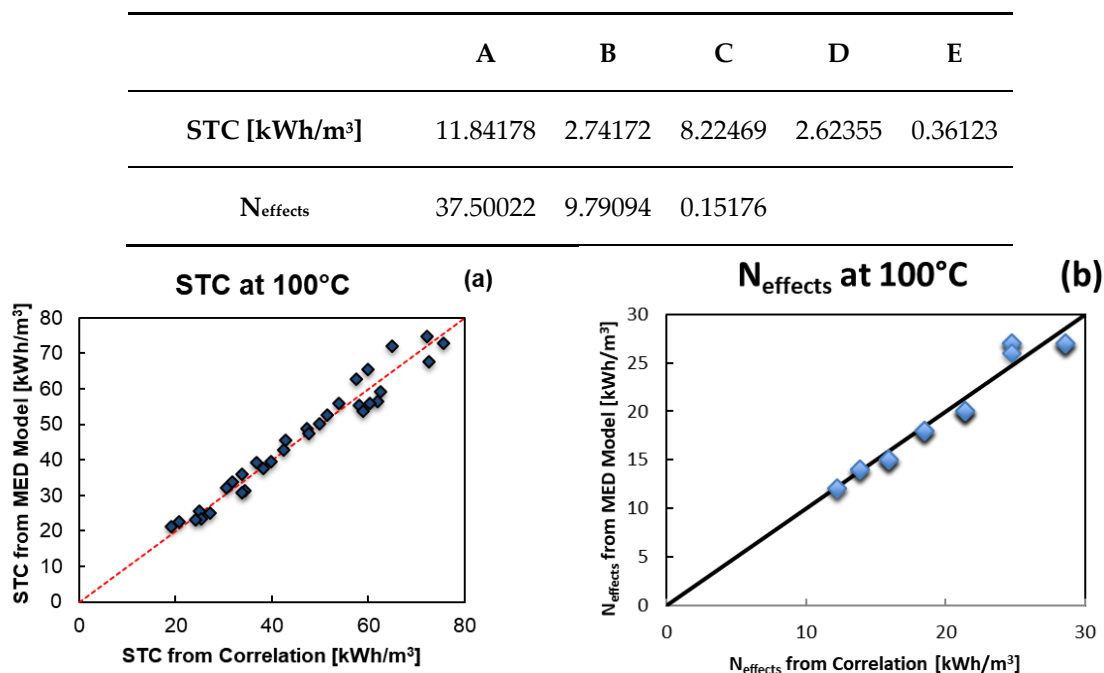


Figure S2.2. Comparison between the MED model predictions and correlation for STC and N_{effect} for the case of waste heat available at 100 °C.

Evaluation of pumping losses in the integrated scheme

Pumping losses in MED unit are evaluated considering:

- The electric power required to pump the inlet solution into the first effect ($P_{MED,in}$).
- The power requirement to pump the distillate and the concentrated solutions from the MED unit to the RED stack ($P_{MED,out}$).
- The pumping power of cooling water required in the final condenser (P_{cond}).

The MED plant is assumed as a vertical plant and each effect is supposed to have a height of 1 m. The $P_{MED,in}$ is given by the product of the solution flow rate ($Q_{MED,in}$) by the hydraulic head (ΔP_{MED}), which depends on the number of effects.

$$P_{MED,in} = \frac{Q_{MED,in} \cdot \Delta P_{MED}}{\eta_{pump}} = Q_{MED,in} \frac{N \cdot \rho_{MED,in} \cdot g \cdot H_{effect}}{\eta_{pump}} \quad (S3.1)$$

Concerning ($P_{MED,out}$); pressure increase ($\Delta P_{MED-RED}$) of 1 bar has been assumed, as the last effect of the MED unit operates at low vacuum conditions (about 50 mbar).

$$P_{MED,out} = \frac{(Q_{H,in} + Q_D) \cdot \Delta P_{MED-RED}}{\eta_{pump}} \quad (S3.2)$$

The pressure drop inside the condenser (ΔP_{cond}) is assumed equal to 0.5 bar while the cooling water flow rate (Q_{cw}), available at 20 °C, is evaluated according to Eq. (S3.4), assuming that in the last effect the distillate is equal to 1/N of the global distillate flow rate (Q_D). Also, a temperature increase of the cooling water (T_{cw}) of 10 °C in the condenser is assumed.

$$P_{cond} = \frac{Q_{cond} \cdot \Delta P_{cond}}{\eta_{pump}} \quad (S3.3)$$

$$Q_{cw} = \frac{\lambda_w \cdot Q_D}{N_{effects}} \cdot \frac{1}{\bar{c}_p(T_{cw,out} - T_{cw,in})} \quad (S3.4)$$

The total pumping power consumption of the MED unit is evaluated according to:

$$P_{MED} = P_{MED,in} + P_{MED,out} + P_{cond} \quad (S3.5)$$

References

- Geise, G. M.; Cassady, H. J.; Paul, D. R.; Logan, B. E.; Hickner, M. A.; Logan, E.; Hickner, M. A. Specific ion effects on membrane potential and the permselectivity of ion exchange membranes. *Phys. Chem. Chem. Phys.* **2014**, *16*, 21673–21681, doi:10.1039/C4CP03076A
- Rottiers, T.; Staelen, J. De; Bruggen, B. Van Der; Pinoy, L. Permselectivity of cation-exchange membranes between different cations in aqueous alcohol mixtures. *Electrochim. Acta* **2016**, *192*, 489–496, doi:10.1016/j.electacta.2016.02.017.
- Gurreri, L.; Tamburini, A.; Cipollina, A.; Micale, G.; Ciofalo, M. CFD prediction of concentration polarization phenomena in spacer- filled channels for reverse electrodialysis. *J. Memb. Sci.* **2014**, *468*, 133–148, doi:10.1016/j.memsci.2014.05.058.
- Vermaas, D. A.; Guler, E.; Saakes, M.; Nijmeijer, K. Theoretical power density from salinity gradients using reverse electrodialysis. *Energy Procedia* **2012**, *20*, 170–184, doi:10.1016/j.egypro.2012.03.018.
- Lakshminarayanaiah, N. Transport phenomena in artificial membranes. *Chem. Rev.* **1965**, *65*, 491–565, doi:10.1021/cr60237a001.
- Gurreri, L.; Tamburini, A.; Cipollina, A.; Micale, G.; Ciofalo, M. Flow and mass transfer in spacer- filled channels for reverse electrodialysis: a CFD parametrical study. *J. Memb. Sci.* **2016**, *497*, 300–317, doi:10.1016/j.memsci.2015.09.006.
- Veerman, J.; Saakes, M.; Metz, S.J.; G.J., H. Reverse electrodialysis: A validated process model for design and optimization. *Chem. Eng. J.* **2011**, *166*, 256–268, doi:10.1016/j.cej.2010.10.071.
- Tedesco, M.; Cipollina, A.; Tamburini, A.; Bogle, I.D.L.; Micale, G. A simulation tool for analysis and design of reverse electrodialysis using concentrated brines. *Chem. Eng. Res. Des.* **2015**, *93*, 441–456, doi:10.1016/j.cherd.2014.05.009.
- Bockris, J. O. M.; Reddy, A. K. N. *Modern Electrochemistry Vol. 1. Ionics*; Springer, Ed.; 2nd ed.; 1998;
- Gurreri, L.; Tamburini, A.; Cipollina, A.; Micale, G. CFD analysis of the fluid flow behavior in a reverse electrodialysis stack. *Desalin. Water Treat.* **2012**, *48*, 390–403, doi:10.1080/19443994.2012.705966.
- Ortega-Delgado, B.; García-Rodríguez, L.; Alarcón-Padilla, D.-C. Opportunities of improvement of the MED seawater desalination process by pretreatments allowing high-temperature operation. *Desalin. Water Treat.* **2017**, *97*, doi:10.5004/dwt.2017.21679.
- Pitzer, K.S. Thermodynamics of Electrolytes. I. Theoretical Basis and General Equations. *J. Phys. Chem.* **1973**, *77*, 268–277, doi:10.1021/j100621a026.
- Van Der Stegen, J.H.G.; Weerdenburg, H.; Van Der Veen, A.J.; Hogendoorn, J.A.; Versteeg, G.F. Application of the Pitzer model for the estimation of activity coefficients of electrolytes in ion selective membranes. *Fluid Phase Equilib.* **1999**, *157*, 181–196, doi:10.1016/S0378-3812(99)00044-8.
- Pitzer, K.S. Electrolyte Theory-Improvements since Debye and Huckel. *Acc. Chem. Res.* **1977**, *10*, 371–377, doi:10.1021/ar50118a004.
- Jones, G.; Bickford, C.F. The Conductance of Aqueous Solutions as a Function of the Concentration. I. Potassium Bromide and Lanthanum Chloride. *J. Am. Chem. Soc.* **1934**, *56*, 602–611.
- Micari, M.; Bevacqua, M.; Cipollina, A.; Tamburini, A.; Van Baak, W.; Putts, T.; Micale, G. Effect of different aqueous solutions of pure salts and salt mixtures in reverse electrodialysis systems for closed-loop applications. *J. Memb. Sci.* **2018**, *551*, 315–325, doi:10.1016/j.memsci.2018.01.036.
- Cerva, M. La; Liberto, M. Di; Gurreri, L.; Tamburini, A.; Cipollina, A.; Micale, G.; Ciofalo, M. Coupling CFD with a one-dimensional model to predict the performance of reverse electrodialysis stacks. *J. Memb. Sci.* **2017**, *541*, 595–610, doi:10.1016/j.memsci.2017.07.030.

